

# Magnetic properties of ZnO:Co layers obtained by pulsed laser deposition method

IRENEUSZ STEFANIUK<sup>1</sup>, BOGUMIŁ CIENIEK<sup>1,\*</sup>, IWONA ROGALSKA<sup>1</sup>, IHOR S. VIRT<sup>2,1</sup>,  
AGNIESZKA KOŚCIAK<sup>1</sup>

<sup>1</sup>Faculty of Mathematics and Natural Sciences University of Rzeszow, Rzeszow, Poland

<sup>2</sup>The Ivan Franko State Pedagogical University in Drohobycz, Drohobycz, Ukraine

We have studied magnetic properties of zinc oxide (ZnO) composite doped with Co ions. The samples were obtained by pulsed laser deposition (PLD) method. Electron magnetic resonance (EMR) measurements were carried out and temperature dependence of EMR spectra was obtained. Analysis of temperature dependence of the integral intensity of EMR spectra was carried out using Curie-Weiss law. Reciprocal of susceptibility of an antiferromagnetic (AFM) material shows a discontinuity at the Néel temperature and extrapolation of the linear portion to negative Curie temperature. The results of temperature dependence of EMR spectra for the ZnO:Co sample and linear extrapolation to the Curie-Weiss law indicated the AFM interaction between Co ions characterized by the Néel temperatures  $T_N = 50$  K and  $T_N = 160$  K for various samples. The obtained g-factor is similar to g-factors of nanocrystals presented in literature, and the results confirm that in the core of these nanocrystals Co was incorporated as  $\text{Co}^{2+}$ , occupying  $\text{Zn}^{2+}$  sites in wurtzite structure of ZnO.

Keywords: *electron magnetic resonance; ZnO:Co; diluted magnetic semiconductor; Curie temperature*

## 1. Introduction

Nanosized zinc oxide (ZnO) doped with transition metal (TM) ions may form diluted magnetic semiconductors (DMSs). DMSs can find possible applications in the spin-dependent semiconductor electronics [1] due to the spin-spin exchange interactions between localized magnetic moments and electrons of conduction band [2]. For practical applications, it is a key issue to raise the Curie temperature  $T_C$  of DMSs above room temperature. Room temperature ferromagnetism (FM) has been observed for several magnetically doped materials such as ZnO [3–5]. At room temperature, FM ZnO, especially Co-doped, has been a subject of special interest: this material is optically transparent, with the band gap of 3.3 eV and the exciton binding energy of 60 meV [6]. The existence of FM ordering in Co-doped ZnO was first proposed theoretically. It was attributed to the double exchange interaction between Co ions [7, 8].

Antiferromagnetic (AFM) couplings are preferred between transition metal atoms in Co-doped ZnO, resulting in a spin-glass state. The FM ordering is realized by electron doping, based on first-principles spin density functional calculations [9]. For the AFM properties, CoO phase: a well-known AFM material with the Néel temperature  $T_N$  of 291 K is responsible [10]. In ZnO:Co, only a few films showed FM features, while the others showed spin-glass-like behavior [10].

We have studied magnetic properties of zinc oxide composite doped with high concentrations of Co. The pulsed laser deposition method (PLD) was used to produce the samples on sapphire substrates ( $\text{Al}_2\text{O}_3$ ).

In the present study, we report electron magnetic resonance (EMR) properties of ZnO:Co layers. The measurements of temperature dependence of EMR spectra were performed. Analysis of the temperature dependence of the integral intensity of EMR spectra was carried out using the Curie-Weiss law.

\*E-mail: cieniek@if.univ.rzeszow.pl

### 1.1. Crystal structure of ZnO

ZnO has three crystal forms: hexagonal wurtzite, cubic zinc blende and cubic rock salt which is rarely observed. The wurtzite structure is most commonly used as it has the highest stability under normal working conditions.

ZnO has stable lattice parameters of wurtzite structure  $a = 0.3296$  nm and  $c = 0.52065$  nm (hexagonal crystal system, P63mc space group) [11]. The structure of ZnO consists of alternating planes composed of  $O^{2-}$  and  $Zn^{2+}$  ions which are tetrahedrally coordinated and stacked along the  $c$ -axis on an alternate basis (Fig. 1). The  $Zn^{2+}$  and  $O^{2-}$  ions create a normal dipole moment and instant polarization which results in diversification of surface energy. The tetrahedral coordination in ZnO results in noncentral symmetric structure, and consequently, in piezoelectricity and pyroelectricity in ZnO. Hexagonal and zinc blende structures do not show inversion symmetry which is a property like these that are responsible for the piezoelectricity and pyroelectricity of ZnO.

Because  $Co^{2+}$  ions have a smaller ionic radius ( $0.58$  Å) than  $Zn^{2+}$  ions ( $0.60$  Å), a substitution of  $Zn^{2+}$  by  $Co^{2+}$  in ZnO lattice matrix in the wurtzite structure is possible [12, 13].

In wurtzite materials like ZnO, substitutional impurities are subjected to a trigonal crystal field. Via the spin-orbit interaction, this anisotropic crystal field induces a strong magnetic anisotropy which can be described by a zero-field splitting (ZFS) of the fundamental state and by an anisotropic effective  $g$ -factor in an effective spin Hamiltonian  $H_s$  in the form:

$$H_s = \mu_B g_{\parallel} H_z S_z + \mu_B g_{\perp} (H_x S_x + H_y S_y) + D S_z^2 \quad (1)$$

where  $S$  is the spin quantum number,  $D$  describes zero-field splitting and  $g_{\parallel}$  and  $g_{\perp}$  are the effective  $g$ -factors for directions of magnetic field parallel and perpendicular to the wurtzite  $c$ -axis, respectively.

The zero-field splitting constant for this particular impurity in ZnO is very small. This is typical of  $S = 5/2$  moments (e.g.  $D = -0.0074$  meV for  $Fe^{3+} d^5$  in ZnO [14],  $D = -0.0027$  meV for

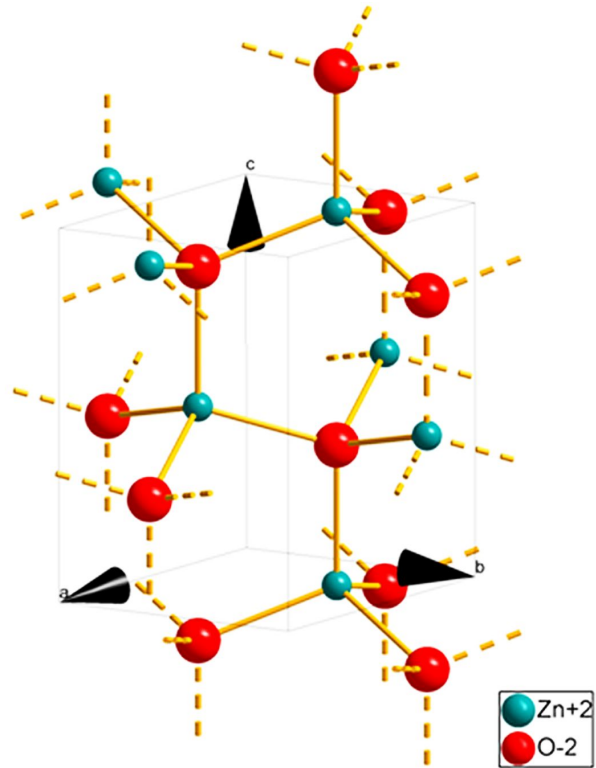


Fig. 1. Crystal structure of zinc oxide (wurtzite).

$Mn^{2+} d^5$  in ZnO [15],  $D = -0.0093$  meV for  $Mn^{2+} d^5$  in GaN [16]), and even for  $Co^{2+}$  ( $d^7$ ,  $S = 3/2$ ) where  $D$  is significantly larger ( $0.342$  meV) [17]. Crystal-field energy level diagram for the effective spin  $S = 3/2$  of the spin-orbit coupling due to large ZFS for the four-coordinated  $Co^{2+}$  ions is presented in Fig. 2.

Due to the very large zero-field splitting, in practice only the transition between spin levels with  $M_s = \pm 1/2$  are possible to observe.

## 2. Experimental

A widely applied in ceramic technology solid state reaction method was used to obtain hard solutions of ZnO:Co. Materials of special cleanness were used as initial components for preparation of the load. The powders of  $CoCO_3$  compounds were obtained by colloidal grinding to the size of particles  $50$  nm to  $100$  nm, and mixed up with small amount of water and ZnO powder in the jasper jar

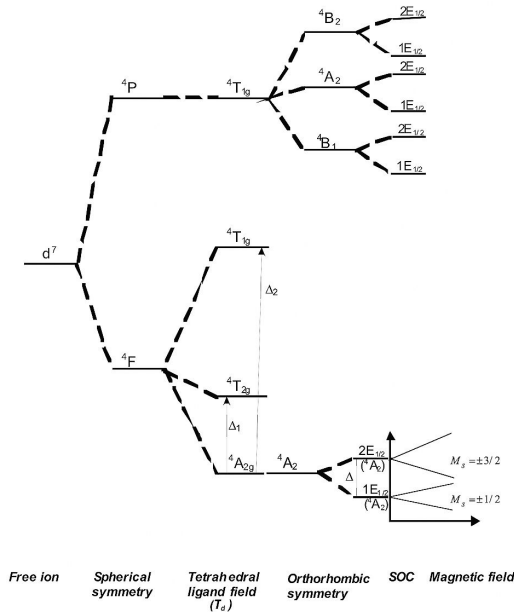


Fig. 2. Crystal-field energy level diagram for the effective spin  $S_{\text{eff}} = 3/2$  of the spin-orbit coupling due to large ZFS for four-coordinated  $\text{Co}^{2+}$  ions.

of a planetary mill SAND-1-1. Time of mixing and grating was determined by the homogenization degree and was set to 16 h. The mixture was dried in a temperature of  $120 \pm 5$  °C.

The mixture was annealed in the chamber furnace VTP-06M1 with periodic operation in two stages. The primary mixture for the activation (decomposition) of  $\text{CoCO}_3$  and doping of the ZnO material was annealed in air at  $700 \pm 5$  °C for 4 hours. Pellets with a diameters of 11.5 mm to 15 mm, 1 mm to 2.5 mm thick were formed by applying pressure of 40 MPa to 60 MPa on a hydraulic press PG-10 without use of plastificators. The pellets were annealed in air for the next 3 hours to improve their mechanical hardness. The accuracy of temperature control was  $\pm 5$  °C. Maximal temperature of annealing, corresponding to the isothermal area of the curve of heating-cooling, was 1110 °C.

Samples of zinc-oxide doped with cobalt on sapphire substrate were prepared by PLD method. The substrate temperature was 200 °C. Beam parameters were as follows: 0.2 nm, 0.5 J in 10 ns pulse, Gaussian distribution, repetition frequency

of 0.3 Hz. Time of a layer growth was about 30 minutes. The layer thickness was 300 nm for sample N88 and 500 nm for sample N79. Concentration of cobalt in both samples was  $x = 4$  % ( $\text{Zn}_{1-x}\text{Co}_x\text{O}$ ).

EMR measurements in the X-band were performed on Bruker multifrequency and multiresonance FT-EPR ELEXSYS E580 spectrometer. The temperature of the samples was controlled in the range of 95 K to 300 K using the Bruker liquid nitrogen gas-flow cryostat with 41131 VT digital controller, and in the range of 4 K to 300 K using the Oxford Instruments ESR 900 liquid helium gas-flow cryostat with Mercury iTC digital controller.

### 3. Results

The EMR spectra of ZnO:Co layers, for samples N79 and N88, are shown in Fig. 3. EMR spectra for both samples consist of a broad line near 1500 Gs and 3300 Gs resulting from  $\text{Co}^{2+}$  ions, and two groups of narrow lines assigned to the impurities in the sapphire substrate, near 2000 Gs (strong intensity), and near 3400 Gs (small intensity).

The EMR features for  $\text{Co}^{2+}$  content smaller than that in our samples should be further split into eight transitions due to hyperfine interaction. However, for higher  $\text{Co}^{2+}$  concentrations,  $x > 0.1$  % [18], only one broad feature related to  $g_{\perp}$  and one broad feature related to  $g_{\parallel}$  were observed. The reported values of  $g_{\perp} = 4.55$  and  $g_{\parallel} = 2.24$  for bulk ZnO:Co and  $g_{\perp} = 4.53$  and  $g_{\parallel} = 2.22$  for thin ZnO:Co film, with the concentration of cobalt of 10 % [18, 19], are similar to  $g$  values obtained by us  $g_{\perp} = 4.56_{\text{N79}}; 4.79_{\text{N88}}$  and  $g_{\parallel} = 2.167_{\text{N79}}; 2.196_{\text{N88}}$ .

In our earlier work we observed EMR signal with  $g \approx 2$  which corresponds to  $g$ -value typical of donors in ZnO [20, 21].

The temperature dependence of EMR spectra for sample N79 is summarized in Fig. 4.

The EMR spectra of impurities and various defects in ZnO show more than ten features in the  $g$ -value range of 1.96 to 2.06. Shallow donors and

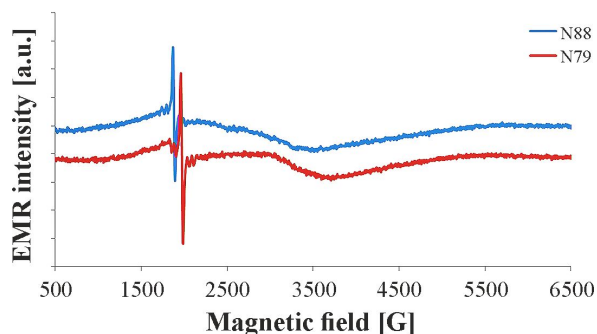


Fig. 3. EMR spectra of ZnO:Co layers (samples N79 and N88) at room temperature.

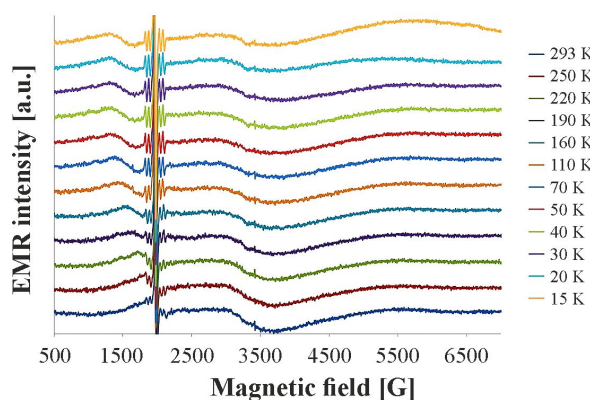


Fig. 4. EMR spectra of the ZnO:Co layer (sample N79).

deep N acceptors are described in the literature as a source of EMR lines with those  $g$ -values [22] (Fig. 4, broad line near 3300 Gs, visible only in low temperatures).

#### 4. Discussion

From the EMR spectra, the effective spectroscopic  $g$ -factor, the peak-to-peak linewidth of the resonance line  $H_{pp}$ , EMR intensity and the resonance field  $H_r$  were determined. Based on these data we obtained the temperature dependencies of  $H_{pp}$  (T), EMR intensity (T),  $g_{\perp}$  (T), and integral intensity as presented in Fig. 5.

Generally,  $Co^{2+}$  ions are characterized by very short spin-lattice relaxation time, therefore their EMR spectra can be clearly observed only at low temperatures (near liquid helium) practically in all crystalline solids according to references

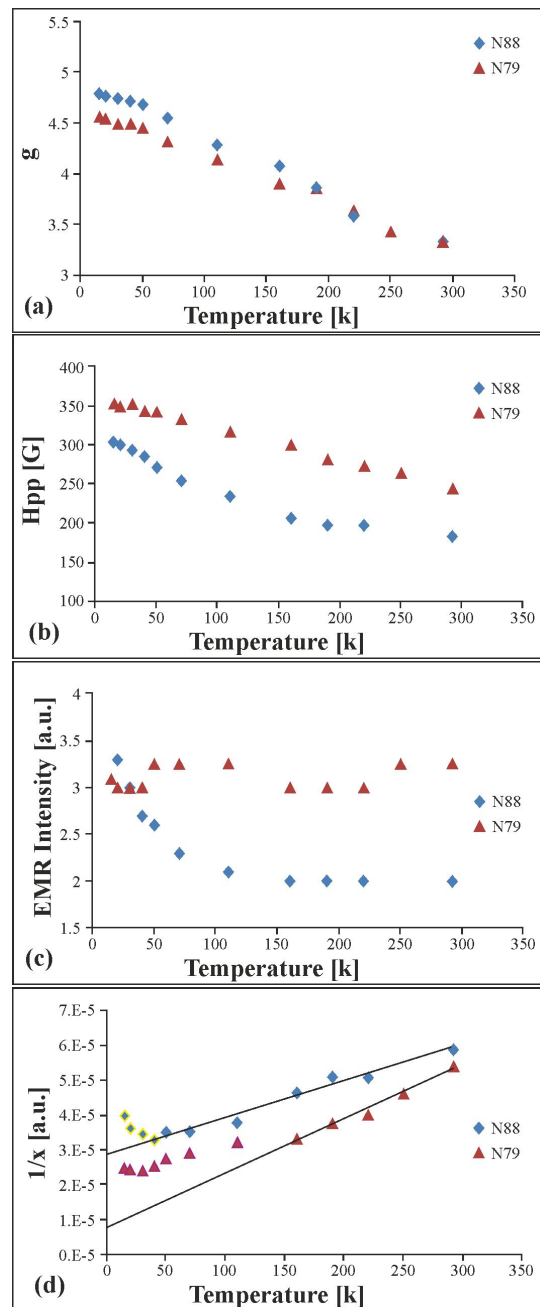


Fig. 5. Temperature dependence of EMR spectra of the sample ZnO:Co (a)  $g_{\perp}$ (T), (b)  $H_{pp}$  (T), (c) EMR intensity (T), and (d) inverse of integral intensity (susceptibility).

data [23–25]. However, in our case we have studied  $Zn_{1-x}Co_xO$  with high concentration of cobalt ( $x = 4\%$ ), therefore we had to take into account magnetic interactions. We observed EMR

lines from helium to room temperature without visible hyperfine structures. This proves the correctness of the assumptions and is consistent with the description of EMR spectra of cobalt ions reported in the literature [26].

We used the Curie-Weiss law to analyse the temperature dependence of the integral intensity, which is directly proportional to the magnetic susceptibility  $\chi$ . A linear increase of  $\chi^{-1}(T)$  at higher temperatures can be fitted to the Curie-Weiss law. Reciprocal of susceptibility of AFM samples showing the discontinuity at the Néel temperature and the extrapolation of the linear portion to the negative Curie temperature are shown in Fig. 5d.

The results of temperature dependence of EMR spectra for the sample ZnO:Co and linear extrapolation to the Curie-Weiss law indicate the AFM interaction between Co ions characterized by the Néel temperatures  $T_{N(N88)} = 50$  K,  $T_{N(N79)} = 160$  K.

The effects of magnetic interactions can be inferred from the magnetization data, but the interaction is AFM and short-ranged. Similar behavior has been observed for Co impurities in ZnO [27–30], which is consistent with the AFM nature of the corresponding oxides FeO and CoO, with Néel temperatures of 198 K and 291 K [31], respectively. This suggests that the localized 3d moments of Co impurities in ZnO can only interact through indirect superexchange via the O2p band, thus excluding all the mechanisms of long-range FM order so far proposed for the wide-gap DMS. The broadening of the CoZn related powder spectrum as the Co-content increases has been already reported in ZnO:Co nanocrystals and it is likely caused by magnetic interaction between neighboring  $\text{Co}^{2+}$  ions.

Considering the structure of ZnO (Fig. 1) and the fact that Co ions substitute the Zn ones, we can presume that the alignment of Co atoms along the c-axis favors the FM state mainly due to weakening of AFM superexchange interactions. The FM state is unlikely to be stabilized because of the very small energy difference between the FM and AFM states. Similar conclusions were presented in

the literature [9], where the calculations indicated that the AFM coupling was more pronounced with increasing Co density.

## 5. Conclusions

In conclusion, we have investigated the nature of magnetic interactions between Co ions in ZnO through EMR measurements. Due to AFM superexchange interactions between Co ions, Co-doped ZnO prefers the spin-glass-like state, while the FM state is stabilized by electron carriers.

Due to high concentration of cobalt ions in  $\text{Zn}_{1-x}\text{Co}_x\text{O}$  ( $x = 4\%$ ) the spectra of cobalt ions  $\text{Co}^{2+}$  in this material are characterized by magnetic interactions over a wide temperature range.

The sample having a smaller thickness (N88) is characterized by more stable parameters which may suggest that the layer has fewer defects (is of better quality).

g-factor obtained in this work is similar to g factor in nanocrystals presented in literature [32]. The results confirm that in the core of these nanocrystals Co has been incorporated as  $\text{Co}^{2+}$ , occupying the  $\text{Zn}^{2+}$  sites in the wurtzite structure of ZnO.

## References

- [1] AWSHALOM D.D., LOSS D., SAMARTH N. (Eds.), *Semiconductors Spintronics and Quantum Computation*, Springer, Berlin, 2002.
- [2] DOBROWOLSKI W., STORY T., *II-VI and IV-VI diluted magnetic semiconductors: New bulk materials and low dimensional quantum structures*, in: BUSCHOW K.H.J. (Eds.), *Handbook of Magnetic Materials vol. 15*, Elsevier, Holland, 2003.
- [3] UEDA K., TABATA H., KAWAI T., *Appl. Phys. Lett.*, 79 (2001), 988.
- [4] READ M.L., EL-MASRY N.A., STADELMAIER H.H., RITUMS M.K., REED M.J., PARKER C.A., ROBERTS J.C., BEDAIR S.M., *Appl. Phys. Lett.*, 79 (2001), 3473.
- [5] CHO S., CHOI S., CHA G.-B., HONG S.C., KIM Y., ZHAO Y.-J., FREEMAN A.J., KETTERSON J.B., KIM B.J., KIM Y.C., CHOI B.-C., *Phys. Rev. Lett.*, 88 (2002), 257203.
- [6] REBIEN M., HENRION W., BÄR M., FISCHER CH.-H., *Appl. Phys. Lett.*, 80 (2002), 3518.
- [7] SATO K., KATAYAMA-YOSHIDA H., *Jpn. J. Appl. Phys.*, Part 2, 39 (2000), L555.

- [8] SATO K., KATAYAMA-YOSHIDA H., *Phys. Status Solidi B*, 229 (2002), 673.
- [9] LEE E.-C., CHANG K.J., *Phys. Rev. B*, 69 (2004), 085205.
- [10] SIEVERS III A.J., TINKHAM M., *Phys. Rev.*, 129 (1963), 1566.
- [11] WANG Z.L., *J. Phys.-Condens. Mat.*, Vol. 16 (2004), R829.
- [12] WU J.J., LIU S.C., YANG M.H., *Appl. Phys. Lett.*, 85 (2004), 1027.
- [13] CUI J.B., GIBSON U.J., *Appl. Phys. Lett.*, 87 (2005), 133108.
- [14] HEITZ R., HOFFMANN A., BROSER I., *Phys. Rev. B*, 45 (1992), 8977.
- [15] CHIKOIDZE E., BARDELEBEN H.J. VON, DUMONT Y., GALTIER P., CANTIN J.L., *J. Appl. Phys.*, 97 (2005), 10D316.
- [16] HEITZ R., THURIAN P., LOA I., ECKEY L., HOFFMANN A., BROSER I., PRESSEL K., MEYER B.K., MOKHOV E.N., *Appl. Phys. Lett.*, 67 (1995), 2822.
- [17] NEY A., KAMMERMEIER T., OLLEFS K., YE S., NEY V., *Phys. Rev. B*, 81 (2010), 054420.
- [18] CASTRO T.J., RODRIGUES P.A.M., OLIVEIRA A.C., NAKAGOMI F., MANTILLA J., COAQUIRA J.A.H., FRANCO A., PESSONI H.V.S., MORAIS P.C., SILVA DA S.W., *J. Appl. Phys.*, 121 (2017), 013904.
- [19] JEDRECY N., BARDELEBEN H.J. VON, ZHENG Y., CANTIN J.-L., *Phys. Rev. B*, 69 (2004), 041308.
- [20] CIENIEK B., STEFANIUK I., VIRT I., *Nukleonika*, 58 (3) (2013), 359.
- [21] STEFANIUK I., CIENIEK B., VIRT I., *Current Topics in Biophysics*, 33 (2010), 221.
- [22] STEHR J.E., MEYER B K., HOFMANN D.M., *Appl. Magn. Reson.*, 39 (2010), 137.
- [23] PIWOWARSKA D., KACZMAREK S.M., BERKOWSKI M., STEFANIUK I., *J. Cryst. Growth*, 291 (2006) 123.
- [24] ALESHKEVYCH P., FINK-FINOWICKI J., SZYM-CZAK H., *Acta Phys. Pol. A*, 111 (1) (2007), 105.
- [25] STEFANIUK I., ROGALSKA I., SUCHOCKI A., BERKOWSKI M., CIENIEK B., POTERA P., *Opt. Appl.*, 44 (1) (2014) 113.
- [26] BARAKI R., ZIEREP P., ERDEM E., WEBER S., GRANZOW T., *J. Phys.-Condens. Mat.*, 26 (2014) 115801
- [27] NEY A., OLLEFS K., YE S., KAMMERMEIER T., NEY V., KASPAR T.C., CHAMBERS S.A., WILHELM F., ROGALEV A., *Phys. Rev. Lett.*, 100 (2008), 157201.
- [28] SATI P., DEPARIS C., MORHAIN C., SCHAFER S., STEPANOV A., *Phys. Rev. Lett.*, 98 (2007), 137204.
- [29] XU Q., ZHOU S., MARKO D., POTZGER K., FASSBENDER J., VINNICHENKO M., HELM M., HOCHMUTH H., LORENZ M., GRUNDMANN M., SCHMIDT H., *J. Phys. D-Appl. Phys.*, 42 (2009), 085001.
- [30] CARVALHO H.B. DE, GODOY M.P.F. DE, PAES R.W.D., MIR M., ORTIZ DE ZEVALLOS A., IIKAWA F., BRASIL M.J.S.P., CHITTA V.A., FERRAZ W.B., BOSELLI M.A., SABIONI A.C.S., *J. Appl. Phys.*, 108 (2010), 079906.
- [31] KITTEL C., *Introduction to Solid State Physics*, Wiley, 8<sup>th</sup> Edition, 2004.
- [32] PEREIRA A.S., ANKIEWICZ A.O., GEHLHOFF W., HOFFMANN A., PEREIRA S., TRINDADE T., GRUNDMANN M., CARMO M.C., SOBOLEV N.A., *J. Appl. Phys.*, 103, (2008), 07D140.

Received 2017-07-13  
Accepted 2017-12-15